ChemComm

COMMUNICATION

View Article Online
View Journal | View Issue

Cite this: *Chem. Commun.*, 2025, **61**, 4403

Received 13th January 2025,
Accepted 17th February 2025

DOI: 10.1039/d5cc00196j

rsc.li/chemcomm

A sensitive fluorescent nanoprobe for sulfatase detection and imaging in living cells and *in vivo*†

Huijia Liu,‡ Jiaqi Zhang,‡ Li Liu, Wenqing Li, Jing Yang* and Peng Wang *

In this study, we developed a fluorescent probe TCF-SULF for sulfatase detection with satisfactory selectivity and sensitivity. After being encapsulated by the DSPE-PEG$_{2000}$, the nanoprobe TCF-SULF NPs can be applied to imaging endogenous sulfatase in MCF-7 cells with low cytotoxicity. Importantly, TCF-SULF NPs were successfully used to monitor sulfatase *in vivo*.

Sulfatases are a class of proteases that are essential to biological organisms because they have the ability to hydrolyze sulfate esters. Currently, scientists have identified 17 genes associated with sulfatases, including ARSA, ARSB, and ARSC.[1] The enzymes encoded by these genes play key roles in biological processes such as hormone synthesis, glycosaminoglycan, and glycolipid metabolism.[2,3] Sulfatase dysregulation is intimately linked to the onset and progression of cancer.[4,5] Steroid sulfatase overexpression, for instance, may promote the desulfation of estrone 3-sulfate, raising estrone levels and potentially causing breast cancer.[6–8] Therefore, sulfatase as a biomarker for cancer detection has become a hot topic of interest in recent years.

The methods used to detect sulfatase mainly include immunoassays,[9] fluorescent probes,[10–12] gas chromatography-mass spectrometry (GC-MS),[13] and analytical isotachophoresis.[14] Among these, fluorescent probes have garnered a lot of interest due to their high sensitivity, low cost, and great selectivity.[15] Currently, numerous fluorescent probe series have been created for sulfatase imaging both *in vitro* and *in vivo*.[11,16–18] *p*-Nitrobenzene sulfate (*p*-NPS), and 4-methyl-umbelliferous sulfate (4-MUS) have been used for commercialization. Although these advanced probes exhibit excellent practical performance *in vitro*, they face challenges when monitoring sulfatase activity under live-cell conditions.[8] The intricate environment found in living cells may have impacts on the probe's stability and reaction efficiency, leading to subpar monitoring outcomes. Thus, a pressing technical challenge in this area is how to modify probes to fit the complex environment inside living cells while preserving their sensitivity and specificity.

Here, we designed a fluorescent probe TCF-SULF, which uses the TCF fluorescent part and a sulfatase-cleavable unit. In the presence of sulfatase, the probe TCF-SULF exhibits a 778-fold increase in fluorescence intensity *in vitro*, and it has high specificity, enabling the specific detection of sulfatase activity. With a determined LOD of 2.12×10^{-3} U mL^{-1}, the probe TCF-SULF demonstrates adequate sensitivity and selectivity towards sulfatase. This probe not only maintains stability in the live cell environment but also exhibits significant fluorescence signal changes based on the presence and activity levels of sulfatase. Therefore, this probe can be utilized for the activity screening of live cells. Importantly, the TCF-SULF probe was effectively utilized for non-invasive observation and documentation of the dynamic changes in sulfatase activity at the tumor site through intratumoral injection in the subcutaneous MCF-7 xenograft model.

TCF-OH is a donor–π–acceptor (D–π–A) structure with strong fluorescence. In the probe TCF-SULF we designed, the sulfate part acts as a recognition group and a protecting group to lock the phenolic hydroxyl of TCF-OH, causing the ICT effect to be interrupted and the photonic signal to be quenched. TCF-SULF can release TCF-OH under the catalysis of sulfatase, thereby achieving the purpose of detecting sulfatase.

The synthetic route is outlined in Scheme 1. According to previous reports, the starting materials 3-hydroxy-3-methyl-2-butanone and malononitrile could form the tricyanofuran intermediate in the presence of EtONa. Then, the tricyanofuran compound was reacted with 4-hydroxybenzaldehyde to give the fluorophore TCF-OH. Finally, the phenolic hydroxyl group of TCF-OH was sulfonated to afford the probe TCF-SULF. All synthesized compounds were characterized using ^{1}H NMR, ^{13}C NMR, and MS.

We evaluated the spectral properties of the probe TCF-SULF in PBS solution (1% DMSO, 10 mM, pH = 7.4). In the absence of sulfatase, TCF-SULF exhibited an absorption peak at 400 nm. However, after adding sulfatase, the absorption peak red-shifted,

Department of Biomedical Engineering, School of Engineering, China Pharmaceutical University, Nanjing 210009, China. E-mail: wangpeng@cpu.edu.cn, yangjing@cpu.edu.cn

† Electronic supplementary information (ESI) available. See DOI: https://doi.org/10.1039/d5cc00196j

‡ These authors contributed equally.

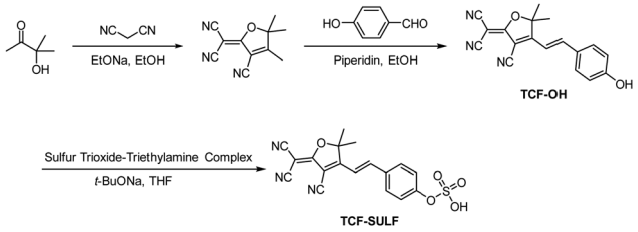

Scheme 1 The synthesis route of the probe TCF-SULF.

and a new absorption peak appeared at 580 nm (Fig. 1a). At the same time, under 580 nm excitation, the fluorescence emission at 620 nm was significantly enhanced (Fig. 1b). Moreover, the fluorescence quantum yield increased to 4.82% after the probe TCF-SULF responded to sulfatase. Therefore, the probe TCF-SULF can be used as a tool to detect sulfatase.

An important parameter to consider for enzyme-activated fluorescent probes is their time response. Under the conditions of 37 °C, the response time of sulfatase and the probe in PBS buffer solution was studied (Fig. S1, ESI†). When sulfatase (20 U mL^{-1}) was present, a significant enhancement in the fluorescence signal could be detected within 2 minutes, indicating that the probe TCF-SULF had a rapid response capability to sulfatase (under 5 minutes). During the 0–30 min period, the fluorescence intensity continuously increased over time, reaching equilibrium at 30 minutes. This indicated the rapid response of the probe TCF-SULF to sulfatase.

We investigated the fluorescence spectrum of TCF-SULF in the presence of different concentrations of sulfatase. When the concentration of sulfatase (0–45 U mL^{-1}) increased, the fluorescence of TCF-SULF at 620 nm was significantly enhanced (Fig. 2a). The fluorescence intensity at 620 nm and the sulfatase concentration (0–10 U mL^{-1}) exhibited an excellent linear connection in the probe–sulfatase reaction, with R^2 = 0.996 (Fig. 2b). This indicated that the probe TCF-SULF had a satisfactory sensitivity for sulfatase detection. Furthermore, using the formula LOD = $3\sigma/k$, it was found that the detection limit of the probe could be as low as 2.12×10^{-3} U mL^{-1}, where σ represents the standard deviation of the blank measurement, and k represents the slope of the fluorescence intensity *versus* sulfatase concentration.

To validate the specificity of the probe, various interfering substances were introduced into the PBS solution containing TCF-SULF (1% DMSO, 10 mM, pH = 7.4) to assess the

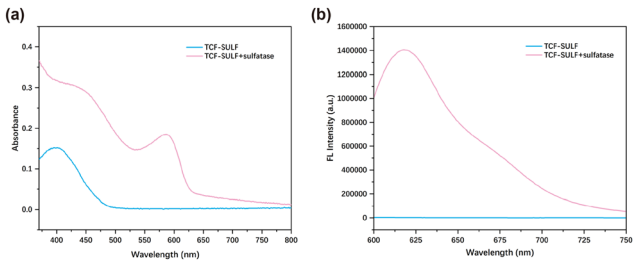

Fig. 1 (a) Absorption spectra of TCF-SULF (10 μM), and TCF-SULF (10 μM) after the addition of sulfatase (20 U mL^{-1}) in PBS solution (1% DMSO, pH = 7.4). (b) Fluorescence spectra of TCF-SULF (10 μM) in the absence and presence of sulfatase (20 U mL^{-1}) in PBS solution (1% DMSO, pH = 7.4).

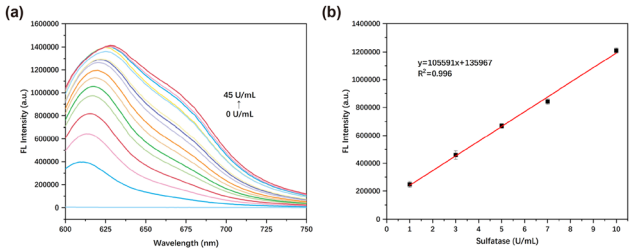

Fig. 2 (a) Fluorescence spectra of TCF-SULF (10 μM) after the addition of various concentrations of sulfatase (0–45 U mL^{-1}) in the inset at 37 °C for 30 min in PBS solution (1% DMSO, pH = 7.4). (b) Sulfatase concentration-dependent fluorescence intensity enhancement of TCF-SULF. $\lambda_{ex}/\lambda_{em}$ = 580 nm/620 nm.

alterations in the solution's fluorescence. After adding other interfering substances, the fluorescence did not significantly increase. After adding sulfatase, the fluorescence increased by approximately 778 times compared to the blank group (Fig. 3). The research results indicated that, compared to other biomolecules and enzymes, the probe TCF-SULF had a higher selectivity for sulfatase.

When TCF-SULF interacted with sulfatase in a series of buffer solutions with pH values ranging from 3.0 to 10.0, a fluorescence enhancement phenomenon was observed for the probe at pH values of 3.0–8.0 (Fig. S2, ESI†). This phenomenon indicated that even under conditions where physiological parameters changed significantly (such as from acidic to alkaline ranges), TCF-SULF can still react with sulfatase to release fluorophores, thereby exhibiting a fluorescent signal. Therefore, this probe had the potential to be used as a biosensor for real-time monitoring of sulfatase activity changes *in vivo* or *in vitro*.

To deeply explore the activation mechanism of the probe TCF-SULF with sulfatase, we specifically conducted a docking study with sulfatase (PDB: 1AUK). The docking results revealed that TCF-SULF can easily embed itself into the hydrophobic cavity of the sulfatase (Fig. 4). It is worth noting that the anionic sulfate group of TCF-SULF was cleverly encapsulated within a catalytic pocket formed by two positively charged residues (Lys123 and Lys302). This structural adjustment significantly shortened the distance between them, thereby greatly enhancing the efficiency of

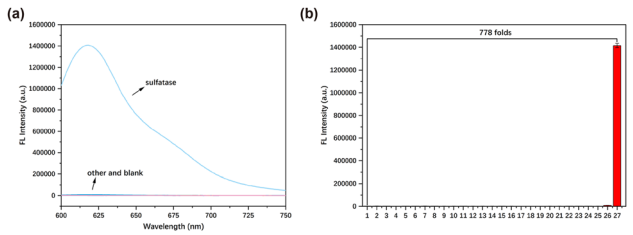

Fig. 3 (a) Probe TCF-SULF (10 μM) in PBS buffer (1% DMSO, 10 mM, pH = 7.4) fluorescence intensity changes for various analytes. (b) Bar chart of fluorescence intensity changes of TCF-SULF in PBS buffer for different analytes. 0: blank, 1: Na^+, 2: Cl^-, 3: Mg^{2+}, 4: K^+, 5: I^-, 6: CH_3COO^-, 7: $HCO3^-$, 8: CO_3^{2-}, 9: HPO_4^{2-}, 10: H_2PO^{4-}, 11: SO_4^{2-}, 12: H_2O_2, 13: NaClO, 14: GSH, 15: Cys, 16: Gly, 17: BSA, 18: DTT, 19: Vitamin C, 20: Glu, 21: Arg, 22: GOX, 23: LOX, 24: Trypsin, 25: β-GC, 26: NADPH, 27: SULF.

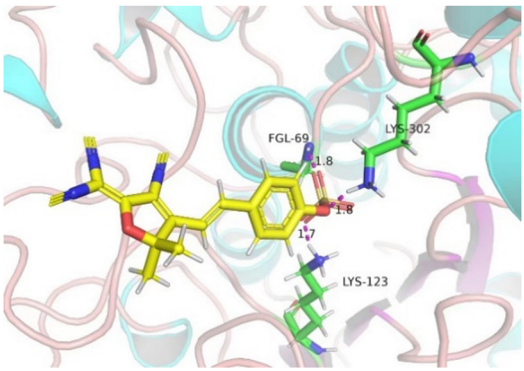

Fig. 4 The binding site between TCF-SULF and sulfatase (PDB: 1AUK). The hydrogen bonds between the three residues (FGL69, Lys123, and Lys302) are represented in red.

the hydrolysis reaction. Furthermore, the sulfate group of the probe formed stable hydrogen bond interactions with other key residues including FGL69, Lys123, and Lys302, which was consistent with previous research reports.[19,20] This indicated that the sulfate ester group played a crucial role in the recognition and binding process with sulfatases, primarily through hydrogen bond interactions.

As shown in Scheme 2, the sensing mechanism of TCF-SULF for sulfatase. When TCF-SULF and sulfatase came into contact, their fluorescence and UV absorption spectra coincided, indicating that the reaction of TCF-SULF with sulfatase resulted in the release of the fluorophore TCF-OH (Fig. S3, ESI†). The identical peak as the TCF-OH molecular weight was seen at *m/z* 302.28 when the product was described using mass spectrometry (Fig. S4, ESI†). Thus, providing more evidence for the expected response mechanism.

To enhance the cell membrane permeability, probe TCF-SULF was encapsulated with DSPE-PEG2000 to afford the nanoprobe TCF-SULF NPs. Using a Malvern particle size analyzer and transmission electron microscopy techniques, a detailed characterization study of the nanoprobes was conducted (Fig. S5, ESI†). The hydrated average particle size of the TCF-SULF NPs reached 159 nm, while the PDI value was 0.227, indicating that the nanoprobes belong to a system with moderate dispersion and maintain an ideal distribution state. Further observation of the transmission electron microscope results revealed that the nanoparticles exhibited a perfect spherical shape and uniform size, approximately 50 nm.

Before bioimaging TCF-SULF NPs in living cells, the cytotoxicity of TCF-SULF NPs on MCF-7 cells was evaluated using the MTT assay (Fig. S6, ESI†). Over 80% of MCF-7 cells were still alive after a 24-hour incubation period, suggesting that TCF-SULF NPs exhibited low cytotoxicity and were suitable for application *in vivo* and in living cells.

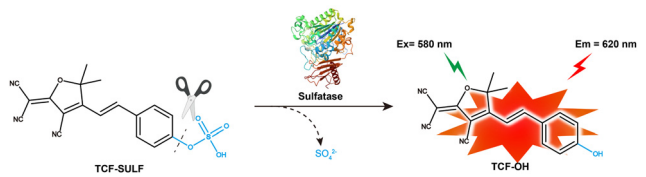

Scheme 2 The proposed reaction mechanism for probe TCF-SULF towards sulfatase.

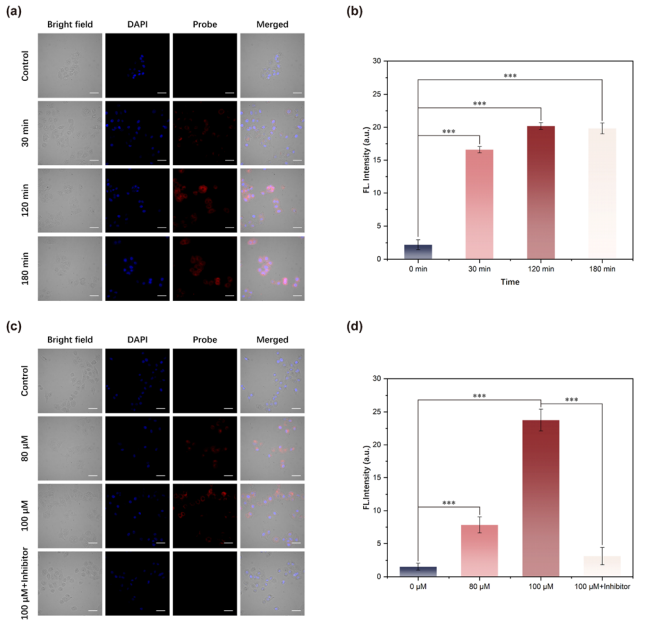

Fig. 5 (a) Fluorescence images of MCF-7 cells incubated with TCF-SULF (100 μM) at different times (0, 30 min, 120 min, and 180 min). (b) Quantification of cellular fluorescence intensity. (c) Fluorescence images of MCF-7 cells co-cultured with TCF-SULF NPs at different concentrations. (d) Quantification of cellular fluorescence intensity. Scale bar = 30 μm; differential analysis was conducted using one-way ANOVA, ***$p < 0.001$.

After co-incubating TCF-SULF NPs with cells for 0.5 hours, red fluorescence can be observed within the cells. The fluorescence signal increased with time and stabilized after approximately 2 hours of incubation (Fig. 5a and b). It indicated the potential of the probe TCF-SULF NPs to enable long-term detection of sulfatase. MCF-7 cells were incubated with different concentrations of TCF-SULF NPs (0, 80, and 100 μM) for 2 hours, rinsed with PBS buffer solution after incubation, and then the nuclei were counterstained with DAPI and imaged under an inverted fluorescence microscope (Fig. 5c and d). As the probe concentration increased, the intracellular fluorescence signal gradually intensified, while cells pre-incubated with the esterase inhibitor showed a significant reduction in intracellular fluorescence signal. This indicated the ability of the probe TCF-SULF NPs to specifically detect sulfatase.

To further explore the imaging potential of TCF-SULF NPs on sulfatase overexpression in mouse tumors *in vivo*, a mouse xenograft tumor model was created by transplanting MCF-7 cells (1×10^6 cells) overexpressing sulfatase into the left axilla of female nude mice. After tumor formation, anesthesia was applied to the mice. After anesthesia, TCF-SULF NPs (400 μM, 50 μL) were injected into the tumor, and *in vivo* imaging of the nude mice was performed using a small animal imaging system (Fig. 6a). Due to the rapid cleavage of sulfate ester bonds by sulfatase, strong fluorescence was observed at the tumor site

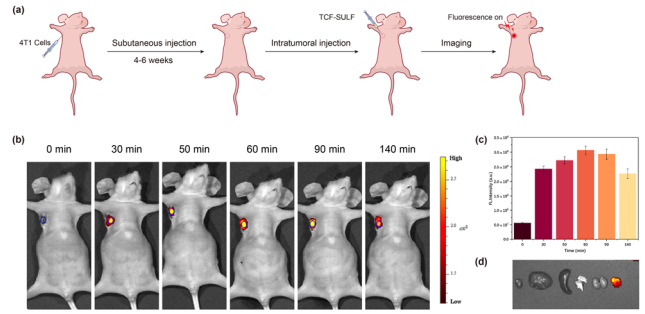

Fig. 6 (a) Imaging study of endogenous sulfatase activity in nude mice with MCF-7 cell xenograft tumors, using TCF-SULF NPs (400 μM, 50 μL) for intertumoral injection. (b) Time-dependent fluorescence imaging and statistical fluorescence intensity. (c) Fluorescence semi-quantitative analysis. (d) *In vitro* organ and tumor imaging.

after 30 minutes, reaching its peak at 60 minutes, accompanied by a high tumor-to-normal tissue (T/N) ratio (Fig. 6b and c). The organs were imaged *in vitro* after the mice were put to sleep. Using fluorescence imaging, tumor tissue with a T/N ratio of 6 could be easily identified from other organs (Fig. 6d). Therefore, the nano TCF-SULF NP probe could serve as an auxiliary tool for resection of the tumor as a contrast agent.

In summary, we have designed and synthesized a TCF-based NIR fluorescent probe TCF-SULF, which uses sulfate esters as recognition sites and exhibits high selectivity and sensitivity towards sulfatase in PBS buffer. Compared to the buffer without sulfatase, the fluorescence intensity increased by 778 times, with an LOD of 2.1×10^{-3} U mL^{-1}. Moreover, the probe has low cytotoxicity and can effectively image the overexpressed sulfatase in MCF-7. Importantly, in the mouse xenograft model, the probe TCF-SULF is capable of imaging tumors. Given its excellent properties, TCF-SULF is expected to become a promising tool for monitoring sulfatases.

We acknowledge funding support from the National Natural Science Foundation of China (NSFC 82071979 and 82202237).

Data availability

The data supporting this article have been included as part of the ESI.†

Conflicts of interest

There are no conflicts to declare.

Notes and references

1 D. Ghosh, *Cell. Mol. Life Sci.*, 2007, **64**, 2013–2022.
2 R. Hobkirk, *Trends Endocrinol. Metab.*, 1993, **4**, 69–74.
3 M. Morimoto-Tomita, K. Uchimura, Z. Werb, S. Hemmerich and S. D. Rosen, *J. Biol. Chem.*, 2002, **277**, 49175–49185.
4 R. Shah, J. Singh, D. Singh, A. S. Jaggi and N. Singh, *Eur. J. Med. Chem.*, 2016, **114**, 170–190.
5 M. Sinreih, T. Knific, M. Anko, N. Hevir, K. Vouk, A. Jerin, S. Frković Grazio and T. L. Rižner, *Front. Pharmacol.*, 2017, **8**, 368.
6 D. J. Ye, Y. J. Kwon, S. Shin, H. S. Baek, D. W. Shin and Y. J. Chun, *Biomol. Ther.*, 2017, **25**, 321–328.
7 P. Nussbaumer and A. Billich, *Med. Res. Rev.*, 2004, **24**, 529–576.
8 H. Y. Yoon, J. H. Lee, S. B. Park, S.-H. Choi, J.-S. Lee and J.-I. Hong, *Dyes Pigm.*, 2022, **205**, 110517.
9 M. P. Cosma, S. Pepe, I. Annunziata, R. F. Newbold, M. Grompe, G. Parenti and A. Ballabio, *Cell*, 2003, **113**, 445–456.
10 H.-J. Park, H.-W. Rhee and J.-I. Hong, *Bioorg. Med. Chem. Lett.*, 2012, **22**, 4939–4941.
11 J. Chen, Z. Peng, M. Ji and P. Wang, *Bioorg. Chem.*, 2023, **138**, 106655.
12 R. Maltais, A. Ngueta Djiemeny, J. Roy, X. Barbeau, J.-P. Lambert and D. Poirier, *Bioorg. Med. Chem.*, 2020, **28**, 115368.
13 T. H. V. Vu, H.-H. Lim and H.-S. Shin, *Bull. Korean Chem. Soc.*, 2020, **41**, 424–432.
14 S. Pajarola, C. Weißenberg, F. Baysal, G. Bruchelt, I. Krägeloh-Mann and J. Böhringer, *J. Chromatogr. B: Biomed. Sci. Appl.*, 2019, **1124**, 109–113.
15 L. Xu, Y. Deng, H. Gao, Y. Yao, X. Liu, W. Zhan, G. Liang and X. Sun, *Nanoscale*, 2024, **16**, 11538–11541.
16 W. Li, S. Yin, X. Gong, W. Xu, R. Yang, Y. Wan, L. Yuan and X. Zhang, *Chem. Commun.*, 2020, **56**, 1349–1352.
17 H.-H. Deng, H.-P. Peng, K.-Y. Huang, S.-B. He, Q.-F. Yuan, Z. Lin, R.-T. Chen, X.-H. Xia and W. Chen, *ACS Sens.*, 2019, **4**, 344–352.
18 Y. Chen, W. Shi, Y. Xu and P. Wang, *Chem. Commun.*, 2023, **59**, 9754–9757.
19 S. R. Hanson, M. D. Best and C.-H. Wong, *Angew. Chem., Int. Ed.*, 2004, **43**, 5736–5763.
20 Y. Xu, M. Cui, W. Zhang, T. Liu, X. Ren, Y. Gu, C. Ran, J. Yang and P. Wang, *Chem. Eng. J.*, 2022, **428**, 132514.

